Development of Targeted Mode for Multi-beamformer Simulation Package

Nishant Deo

Indian Institute for Science Education and Research, Kolkata

Under the Supervision of
Ms.Mekhala Muley

Giant Meterwave Radio Telescope
National Centre for Radio Astrophysics
Tata Institute of Fundamental Research

May 2024 - July 2024

Contents

List of Figures

Acknowledgements

I would like to express my sincere gratitude to all those who have contributed to the successful completion of this project at GMRT (Giant Meterwave Radio Telescope).

First and foremost, I am immensely thankful to my project guide, Ms.Mekhala Muley, for her valuable guidance, constant encouragement, and support throughout the project. Their expertise and insights have been instrumental in shaping this work.

I am deeply grateful towards Dr. Jayanta Roy for giving me the opportunity to this invaluable experience and for his constant guidance.

I extend my thanks to Mr. Ajith Kumar B., Group Coordinator, GMRT Backend Group, for his cooperation, support, and permission to work within the Digital Back-end Group.

I am also thankful to Mr. Sanjay Kudale, Mr. Harshwardhan Reddy, Mr. Ujjwal Panda and Mr. Kenil Ajudiya who provided valuable assistance and support by helping me understand the topic in more detail. Their insights and explanations were invaluable in enhancing my understanding and approach.

I am grateful to the entire team at GMRT for providing me with the necessary resources and facilities to conduct my research. The cooperative environment and expert assistance have been invaluable in the execution of this project.

I would also like to acknowledge the help and support from my colleagues and friends who have provided valuable inputs and feedback during the course of this work.

Abstract

Fast Radio Bursts (FRBs) are millisecond duration highly energetic dispersed radio pulses originating from extragalactic sources. One of the significant challenges in FRB research is their localization. Accurate localization is crucial for identifying host galaxies and understanding the environments in which these bursts occur. Radio Interferometric Array provides higher spatial resolution and tiling the FoV with multiple beams will increase the FRBs survey speed.

Currently at GMRT, the beamformer forms four beams Phased Array, Incoherent Array or both. One of the possibility of improvement in performance is by increasing number of beams. This can be used for implementing different features useful for astronomical studies Radio Frequency Interference mitigation schemes, increasing survey speed for FRBs etc. This gave the motivation to develop a system to form multiple beams using GMRT. So, the multi-beamformer simulation package was developed for sky survey. Currently, at GMRT, we have tested and implemented the multi beamformer code for 100 phased array beams. This code formed 2000 beams, which will be used for Sky survey in the SPOTLIGHT project. SPOTLIGHT is a real-time multi-beam commensal project that will run parallel to regular GMRT observations and will search for FRBs and pulsars within the full-width-half-maximum (FWHM) of the field-of-view (FoV). Multi-beam is part of commensal system which is running in parallel to GWB, hence enhancing the capabilities of GMRT.

Similar kind of work is been carried out across the world. MeerKAT has developed a software package and we have carried a comparative study so that new features can be added based on our science goal. At GMRT, we already implemented the Survey Mode. However, for any specific target study, we

need the Targeted Mode. In this project, this mode was implemented and tuned to satisfy the requirements of SPOTLIGHT.

Further, the parameters like the number of beams, FoV, tiling efficiency were analysed for various antenna configurations. The issue of intrinsic grating lobes was analysed as well and the solution to increase the overlap level was proposed.

Chapter 1

Introduction

1.1 Overview of GMRT

Figure 1.1: GMRT Antennas

The Giant Metrewave Radio Telescope (GMRT) is comprised of 30 antennas, each with a diameter of 45 meters. These antennas are specifically engineered to function across a wide frequency range, spanning from 50 MHz to 1450 MHz. The construction of these antennas involves an innovative approach called the SMART technique, which employs wire mesh panels attached to rope trusses.

1.2 Antenna Configuration

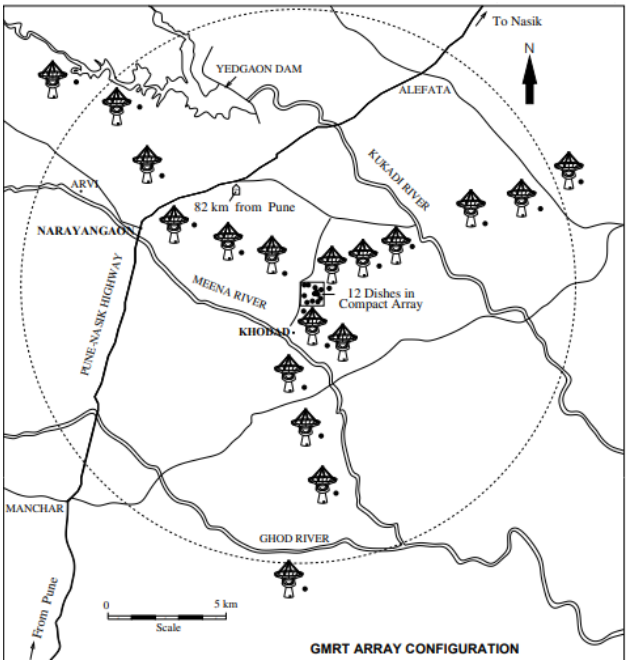

Figure 1.2: GMRT Array Configuration

The GMRT is a radio telescope featuring a hybrid configuration, as depicted in Figure 1.2. In the central square, 14 antennas are randomly distributed within an approximately 1 km area. These central square antennas are denoted as C00, C01, up to C14. Additionally, the GMRT has three arms, namely the East, West, and South arms. Each arm spans about 14 km in length, and antennas are distributed along these arms. They are labeled as E01 to E06 for the East arm, W01 to W06 for the West arm, and S01 to S06 for the South arm. The maximum baseline length between antennas located at the farthest ends of the arms is approximately 25 km.
The design of the GMRT allows it to gather data on various angular scales during a single observation. The central square antennas provide numerous relatively short baselines, making them ideal for imaging large extended sources with visibility concentrated near the origin of the UV plane. On the other hand, the antennas in the arms are beneficial for imaging smaller sources that require high angular resolution.

In summary, the GMRT's hybrid configuration combines the advantages of the central square antennas, which are excellent for imaging extended sources, and the arm antennas, which excel at imaging smaller sources with high resolution. This configuration allows the telescope to capture diverse and valuable information during its observations.

1.3 GMRT Beamformer

A radio interferometric array is primarily designed to map the sky brightness distribution by measuring the instantaneous cross-correlations. In addition to the interferometric imaging mode, such a multi-element radio telescope array is required to be configured to work as a single dish called a 'beamformer' for studying compact objects like pulsars. Beamforming is a signal processing technique which is used for directional signal transmission and reception. It is achieved by combining the signals from elements in a phased array in such a way that signals at particular angles will experience constructive interference while others experience destructive interference. In the GMRT, Beamformer is the stage in the receiver chain where the signals from different antennas, after going through FFT and delay correction, are combined and converted into power.If the voltage signals are added before squaring then it forms Phased Array while otherwise if the signals are first converted into powers and then added, then it forms Incoherent Array, as the phase information is lost now.

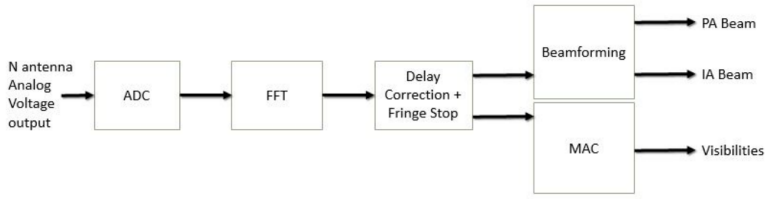

Figure 1.3: Block Chain Diagram for GMRT

1.4 NSM-GMRT

The National Supercomputing Mission (NSM) is funding a project to develop a High-Performance Computing (HPC) facility with PetaFlop computing capacity. Its main purpose is to conduct a real-time commensal search for Fast Radio Bursts (FRBs) and pulsars with the Giant Metrewave Radio Telescope (GMRT).

The HPC facility will process data from the GMRT digitizer outputs at a remarkable rate of 25 GB/s, facilitated by 32 10Gb fiber links, enabling continuous 24/7 data processing. The correlator and beamformer components will create 2000 beams, covering 50% of the telescope's field-of-view using phased addition of visibilities from antennas with moderate baselines. The successful execution of this project will enable transformational, high-impact science in time-domain astronomy with the GMRT along with being a trigger for cutting-edge technology development in the country.

1.5 SPOTLIGHT

FRBs are extremely bright, millisecond duration events detectable at cosmological distances. In addition to being probes of highly energetic, and possibly cataclysmic events, they also provide a unique opportunity to study the intergalactic medium (IGM). Their short duration and often non-repeating nature makes them both difficult to detect and localise. Localising them to arcsecond accuracy or greater helps identify their host galaxies, which allows their use as cosmological probes.

The SPOTLIGHT (**S**urvey for s**P**oradic radi**O** burst**T**s via a commensa**L** mult**I**-beam **G**pu-powered **H**pc at the gmr**T**) project with the GMRT, funded by the National Supercomputing Mission (NSM), is aiming to build a commensal backend to search for FRBs and pulsars using 2000 beams over a frequency range of 300 to 1460 MHz.

Chapter 2

Beam Forming

2.1 Antenna Theory

Antenna is the interface between radio waves propagating through space and electric currents inside a metallic conductor. It is an array of conductors and can be designed in such a way so that it can emit/receive signals in all directions or in a specific direction. The antenna used in GMRT have parabolic reflectors for a directional beam. Directional antennas have high-gain (defined as the ratio of the power in a specific direction to the power by an isotropic antenna) and thus exhibit more power in a specific direction.

The beam of an antenna refers to the radiation pattern of the antenna. For a directional antenna, the beam can be depicted by figure 2.3. This beam of an antenna can be approximated by a Gaussian. The mainlobe is the region consisting of the maximum power, while the other lobes are called sidelobes (grating lobes). Grating lobes can be reduced by changing the weights of the antenna. The antenna weights (gain) can change the beam shape. If the weights are equal then the beam shape will be like a sinc function i.e. main beam with grating lobes. However if a gaussian weight distribution is used it can give a wider beam with no grating lobes. So depending upon the requirement one can digitally control the main beam and grating lobes by providing appropriate weights

2.2 Need of Antenna Array

A single element telescope with a steerable paraboloidal reflecting surface is the simplest kind of radio telescope that is commonly used. We can have a maximum aperture of 100 m due to engineering limitations, which if operating at a wavelength of 1m will give a resolution of 30 arc min, which is much less than normal ground operating optical telescopes. Use of antenna arrays is one way of increasing the effective resolution and collecting area of a radio telescope. An array usually consists of several discrete antenna elements arranged in a particular configuration. The outputs (voltage signals) from the array elements can be combined in various ways to achieve different results.

2.3 Beam Forming Concept

Pulsars are the weak radio sources, so their individual pulses often do not rise above the background noise level. Pulsar is a very highly magnetized rotating neutron star, which emits pulses with a very high precision period i.e small duty cycle. Beamforming is the basic technique used for their studies. It is used in sensor arrays for directional signal transmission or reception. This is achieved by combining elements in the array in such a way that signals at particular angles experience constructive interference while others experience destructive interference. In beamformer, the antenna signals can be added coherently or incoherently. So for Pulsar observation, array mode with higher time resolution is used.

Beam forming refers to the process of combining signals from multiple antennas or sensor elements to create a more focused and directional beam. It aims to maximize the signal power in the desired direction while minimizing interference and noise from other directions. By adjusting the phase and amplitude of the signals received or transmitted by each antenna element, constructive interference is achieved in the desired direction, resulting in enhanced signal strength. Beam forming is used to obtain the desired radiation pattern to achieve specific beam characteristics, such as directionality, beamwidth, and beam shape.

2.4 Types of Array

2.4.1 Phased Array

A phased array is created by combining voltage signals from different antennas after applying appropriate delays and phase adjustments. This synchronized combination is then fed into a square law detector, resulting in an output that is directly proportional to the power of the combined signals. For identical elements, this phased array gives a sensitivity which is N times the sensitivity of a single element, for point source observations. The beam of such a phased array is much narrower than that of the individual elements, as it is the process of adding the voltage signals with different phases from the different elements that produces the narrow beam of the array pattern.

2.4.2 Incoherent Array

An incoherent array operates by directly feeding the voltage signals from N antennas into a square law detector. This process converts the signals to their respective powers. These individual powers are then combined by addition to derive the final output of the array. Unlike a phased array, where signals are carefully combined with precise phase adjustments, the incoherent array's output represents the combined power from all antennas without providing specific directional information or beamforming capabilities. The beam of the resultant telescope has the same shape as that of a single element, since the phases of the voltages from individual elements are lost in the detection process. Also the beamwidth is usually more than that of coherent phased array telescope. The sensitivity in this case is less than that of coherent phased array by a factor of $\sqrt{N}$

2.5 Beam Steering

Beam steering is the process of directing a beam of signals in a specific direction by adjusting the phase and amplitude of the signals in each antenna element or sensor. It is a key application of Beam forming. In traditional fixed antennas, the main radiation beam is fixed in a specific direction, and to change the pointing direction, the entire antenna must physically rotate or move. Phased array antennas consist of multiple individual antenna elements that can be independently fed with different signals and electronically

adjusted in phase and amplitude. By adjusting the signals fed to each element, the antenna system can effectively change the direction of the main beam without physically rotating the antennas.

2.6 Multi-beam Forming

Multi-beam Forming is an advanced technique in signal processing and antenna systems that involves creating and steering multiple simultaneous beams in different directions. Instead of focusing on a single beam, multi-beam forming enables the formation of multiple independent beams, each pointing towards a different target or direction of interest by performing phase adjustments. Each beam can be dedicated to observing a specific region of the sky, thereby allowing for deeper and more focused observations of individual sources. It allows the telescope to access a wider region of sky by allowing to observe multiple regions of the sky simultaneously.

2.7 Science with Multi-beams

Fast Radio Bursts (FRBs) are millisecond duration highly energetic dispersed radio pulses originating from extragalactic sources. One of the significant challenges in FRB research is their localization. Accurate localization is crucial for identifying host galaxies and understanding the environments in which these bursts occur. Radio Interferometric Array provides higher spatial resolution and tiling the FoV with multiple beams will increase the FRBs survey speed. Using multiple beams allows for higher resolution imaging by providing more data points over the observed area. Multi-beam systems can selectively focus on desired signals. Thus, in context of SPOTLIGHT project we can claim that multibeams are helpful in the precise localization of FRBs.

2.8 Beam Forming Theory

2.8.1 The 2 Element Array

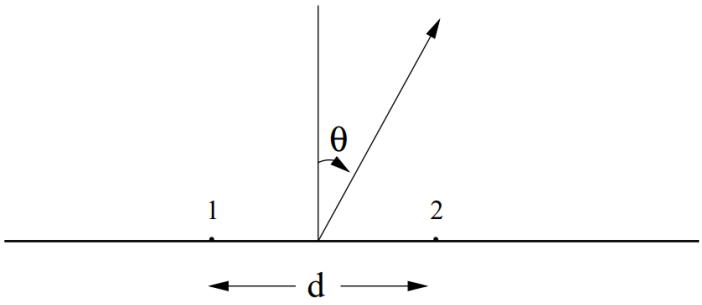

Figure 2.1: Geometry for 2 Element Array

The net far-field in the given direction θ is given as

$$E(\theta) = E_1 e^{\frac{j\psi}{2}} + E_2 e^{-\frac{j\psi}{2}} \tag{2.1}$$

where, $\psi = kdsin\theta + \delta, k = 2\pi/\lambda$ is the wave number and δ is the intrinsic phase difference between the two sources. E_1 and E_2 are the amplitudes of the electric field due to the two sources, at the distant point under consideration. The reference point for the phase, referred to as the phase centre, is taken halfway between the two elements. If the two sources have equal strength, $E_1 = E_2 = E_0$ and we get

$$E(\theta) = 2E_0 cos(\psi/2) \tag{2.2}$$

The power pattern is obtained by squaring the field pattern. $E(\theta)$ also represents the voltage reception pattern obtained when the signals from the two antenna elements are added, after introducing the phase shift δ between them.
Now, we can extend this result to n-Elements of Equal Amplitude and Spacing.

2.8.2 Linear Arrays of n Elements of Equal Amplitude and Spacing

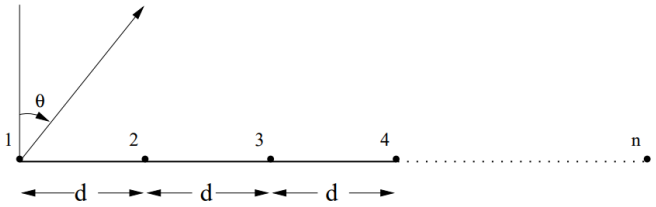

Figure 2.2: Geometry for N Element Array

Taking the first element as the phase reference, the far field pattern is given by

$$E(\theta) = E_0[1 + e^{j\psi} + e^{2j\psi} + \cdots + e^{(n-1)j\psi}] \tag{2.3}$$

where, $\psi = kdsin\theta + \delta, k = 2\pi/\lambda$ is the wave number and δ is the progressive phase difference between the sources. Thus,

$$E(\theta) = E_0 \frac{sin(n\psi/2)}{sin(\psi/2)} e^{j(n-1)\psi/2} \tag{2.4}$$

If the centre of the array is chosen as the phase reference point, then the above result does not contain the phase term of $(n-1)\psi/2$. For non-isotropic but similar elements, E_0 is replaced by the element pattern, $E_i(\theta)$, to obtain the total field pattern.

The field pattern in the above equation has a maximum value of nE_0 for $\psi = 0, 2\pi, 4\pi, \ldots$. The maxima at $\psi = 0$ is called the **main lobe**, while the maxima at $psi = 2\pi, 4\pi, \ldots$ are called as **grating lobes**. By suitable choice of the value of δ, this maxima can be "steered" to different values of θ, using the relation $kdsin\theta = -\delta$.

For non-isotropic elements, the element pattern also needs to be steered (electrically or mechanically) to match the direction of its peak response with that of the peak of the array pattern, in order to achieve the maximum peak of the total pattern.

The uniform, linear array has nulls in the radiation pattern which are given by the condition $\psi = \pm 2\pi l/n, l = 1, 2, 3 \ldots$ which yields

$$\theta = \arcsin\left[\frac{1}{kd}\left(\pm\frac{2\pi l}{n} - \delta\right)\right] \tag{2.5}$$

For a broadside array ($\delta = 0$), these null angles are given by

$$\theta = \arcsin\left(\pm\frac{2\pi l}{nkd}\right) \tag{2.6}$$

Further, if the array is long ($nd \gg l\lambda$), we get

$$\theta \approx \pm\frac{\lambda l}{nd} \approx \pm\frac{l}{L_\lambda} \tag{2.7}$$

L_λ is the length of the array in wavelengths and $L_\lambda = \frac{(n-1)d}{\lambda} \approx \frac{nd}{\lambda}$ for large n The first nulls occur at l = ± 1, and the beam width between first nulls (BWFN) for such an array is given by

$$BWFN = \frac{2}{L_\lambda} rad = \frac{114.6}{L_\lambda} deg \tag{2.8}$$

The half-power beam width (HPBW) is then given by

$$HPBW \approx \frac{BWFN}{2} = \frac{57.3}{L_\lambda} deg \tag{2.9}$$

2.8.3 Power Pattern

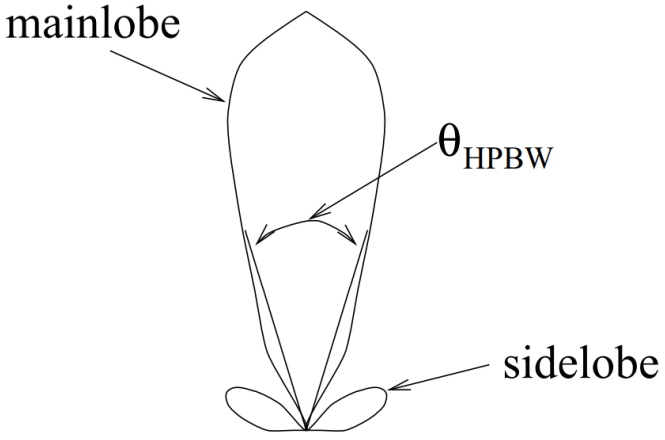

Figure 2.3: Power Pattern of an Antenna

The effective aperture of an antenna is defined as

$$A_e = \frac{\text{Power density available at the antenna terminals}}{\text{Flux density of the wave incident on the antenna}} \tag{2.10}$$

The effective area is a function of the direction of the incident wave, because the antenna works better in some directions than in others.

$$A_e = A_e(\theta, \phi) \tag{2.11}$$

This directional property of the antenna is often described in the form of a power pattern.

$$P(\theta, \phi) = \frac{A_e(\theta, \phi)}{A_e{}^{max}} \tag{2.12}$$

A typical power pattern is shown in figure 2.3. The power pattern has a primary maximum, called the main lobe and several subsidiary maxima, called side lobes. The points at which the main lobe falls to half its central value are called the Half Power points and the angular distance between these points is called the Half Power Beamwidth (HPBW).

2.8.4 SNR Calculation

For one antenna, we know that:

$$\text{SNR} = \frac{P}{\sigma} \tag{2.13}$$

where P is the output power of the antenna and σ is the rms of the power For incoherent array, we have:

$$SNR_{IA} = \frac{\sqrt{N}P}{\sigma} \tag{2.14}$$

For phased array, we have:

$$SNR_{PA} = \frac{NP}{\sigma} \tag{2.15}$$

Thus,

$$\frac{SNR_{PA}}{SNR_{IA}} = \sqrt{N} \tag{2.16}$$

Chapter 3

Multi-beamformer Simulation Package

3.1 Survey Mode

A real-time multi-beamformer code was developed in Python. Using moderate baseline of 23 or lesser antennas, it extracts the beam parameters from the contour plot using central contour extraction from OpenCV library at a constant user defined overlap level. 2000 beams are then arranged in a rectangular fashion in a square FoV and it is ensured that the FoV does not cross the FWHM of primary beam.

Further, for precise localization of source the clustered beams are grouped together into 24 indexes which are then sent to 24 processing units. The final RA-DEC centres are outputted to the user. This code was integrated with the pipeline in C using IPC (Inter-Process Communication), connecting C with Python. Based on the timing analysis of the code and pipeline, it was decided to set an update rate of 1 min for the beam tiling i.e. this code will be called every minute and it will re-arrange the beams and return the new RA-DEC centres every minute.

3.2 New Features and Mode

In this section, I will be introducing the Targeted Mode, the new addition to the Multi-beamformer Simulation package, the purpose of which will be to

study a specific target.

Similar to the Survey Mode, the beam pattern of the variable array is calculated depending on the RA, DEC, date and time of observation. The beam pattern has grating lobes due to unfilled array and hence only central contour is extracted. An ellipse is fitted to the the beam using cv2 and it is ensured that the region inside the ellipse is above 0.5 overlap level. Due to intrinsic grating lobes in lower antenna configurations (14 to 23 antennas), the overlap level is changed accordingly.

3.2.1 Changes in the Survey Mode

Few additions have been made to the Survey Mode to improve the sensitivity and the localization of the source. The beam arrangement was changed from rectangular to shifter rectangular, causing a 3% efficiency improvement. Previously, the beam could be arranged only in rectangular bounding box, but now the beams can be arranged in hexagonal and circular bounding box as well. To incorporate this feature in survey mode furthur work is required for arraning the beams wihtin subeams in clsoe proximity of each other.

3.2.2 Targeted Mode

Survey mode helps in knowing the source's approximate location. Once the approximate location is determined further astronomical studies can be carried out. To carry out such source specific observations, a new mode - Targeted mode is developed in multi-beamformer simulation package. This mode will form few hundreds of beams in the given FoV at 0.5 overlap using full array thus facilitating more precise localisation of the source.

The basic flow remains intact, the calculation of power pattern, beam extraction and then arranging in the appropriate fashion. Similar to the Survey Mode, beams are arranged in a shifted rectangular fashion. The maximum and minimum FoV limit (limitation of the code) is displayed to the user, The beam tolerance (maximum number of beams that can be processed by the system) is inputted by the user. Keeping the overlap level 0.5, the number of beams are determined and the overlap level is tuned such that the number of beams are a multiple of 24.

If the FoV is not filled for 30 antenna, then the number of antennas are reduced to fill in the required field of view. If the number of antennas are less than 23, then the to tackle the intrinsic grating lobes issue, the overlap level is increased, this issue has been analysed rigorously in the 4.3.2 section.

The beams can be arranged in 3 bounding boxes for targeted mode, viz. rectangular (square), circular and hexagonal as shown in figure 3.1, figure 3.2 and figure 3.3. Initially, the beams are arranged in a square with circumradius determined by the bounding box scale. Then, the beams outside the bounding box are removed and if the number of beams inside are not equal to the expected number of beams then the nearest beams are added to make the number of beams equal.

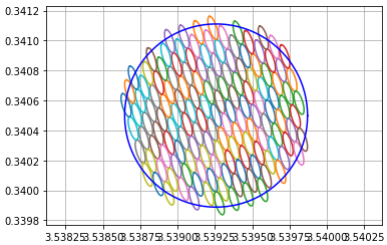

Figure 3.1: 144 Beams in Circular Bounding Box

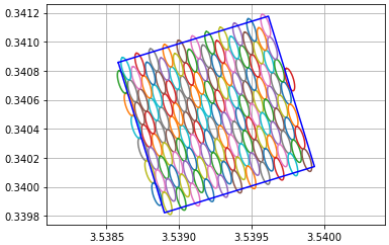

Figure 3.2: 144 Beams in Square Bounding Box

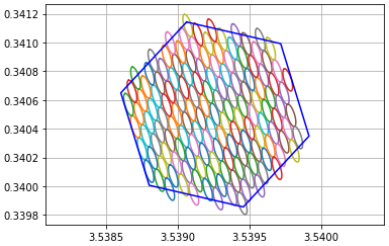

Figure 3.3: 144 Beams in Hexagonal Bounding Box

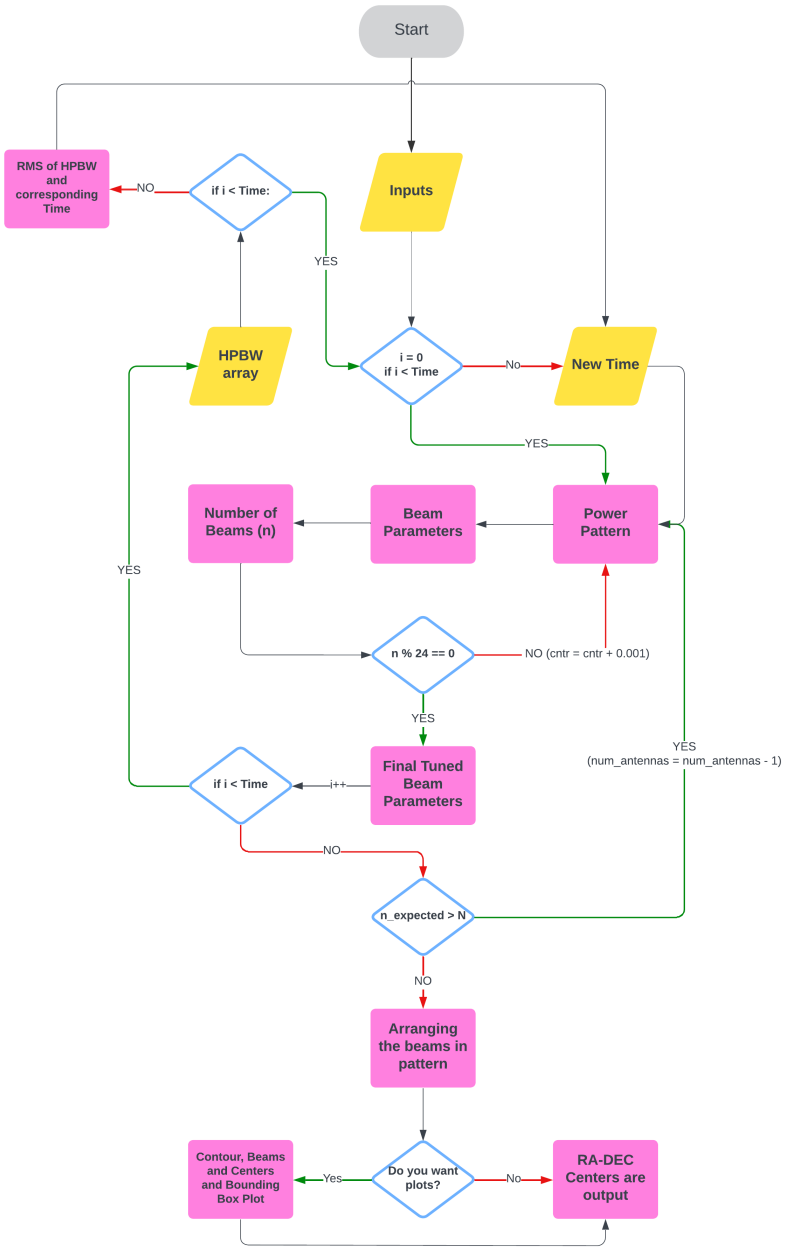

Figure 3.4: Flowchart for Target Mode

3.2.3 Tiling Efficiency

As mentioned in more detail in section3.3.3, re-tiling of beams causes the beams to change tracking position and can be problematic causing data loss and calibration challenge and other complexities in unbroken integration. Thus, it is required to efficiently arrange the beams such that there is minimum sensitivity drop for the entire observation duration. Further, it was hypothesized that the beams are arranged according to an ideal time, such that the efficiency will not drop below a certain threshold. The analysis and comparison for different methods is done in 4.4.

3.3 MeerKAT Widefield Beamforming

MeerKAT is a 64-dish interferometer in the Northern Cape of South Africa, with baselines of up to 8 km and a collecting area of around 9161 m^2. MeerKAT has a beamformer that can generate upto 1000 digitally synthesized beams. It uses voltage beamforming and that apply delay corrections via phase shifting in the Fourier domain. MeerKAT has developed a Python package called MOSAIC for the multibeam formation and tiling.

3.3.1 Beam shape simulation

Provided with an arbitrary set of antenna positions and a source position, the Mosaic package uses a sparse discrete Fourier transform approach to recover the point spread function. By default, Mosaic weights each antenna in the array equally during the generation of the PSF. However, in real observations, the performance of the antennas and the quality of the calibration applied may vary. This results in non-uniform amplitude and phase responses across all antennas, causing the true PSF of the observation to differ from the simulation. The region bounded by a certain response level is irregular thus, it is approximated by an ellipse for later tessellation of beams in a tiling. The beam is simplified by ellipse using the katbeam package.

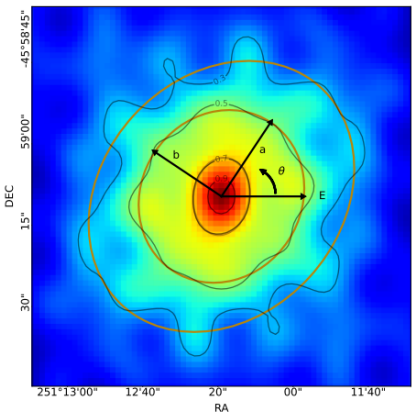

Figure 3.5: Simulated PSF for MeerKAT using 54 antenna, approximating beams at specific levels by an ellipse using katbeam

3.3.2 Beam Tiling

There are two methods to tile the beams depending on whether the user requires a fixed overlap (constant minimum sensitivity) or a fixed boundary of the tiling (constant FoV). With the beam shape approximated as a set of ellipses at different response levels, an efficient tessellation can be achieved through hexagonal packing.

In case of fixed overlap ratio method, the beams can be arranged in 2 bounding boxes, circular and hexagonal. After retrieving the beam parameters, the beams are arranged in a square of side decided by the radius (circumradius in case of hexagon) and then oriented accordingly. The beams outside the bounding box are then removed and then the bounding radius is recalculated until the beam number inside the bounding box is within the tolerance limit of the required number of beams.

In case of constant FoV mode, the user can specify the bounding box to be either of circular, hexagonal, elliptical, annulus or arbitrary polygonal. According to bounding box scale, the tiling module calculates the overlap ratio which is tuned until the number of beams inside is within the tolerance limit. The beams are initially arranged in a square of side determined by the scale of the bounding box and then the beams outside the bounding box are removed.

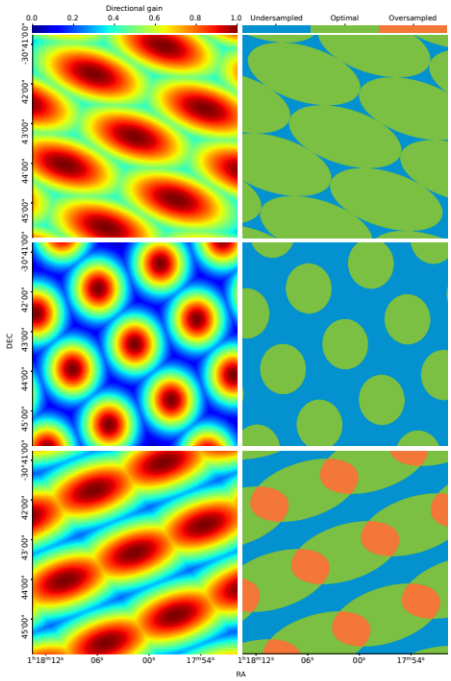

Figure 3.6: Tiling evolution with time, blue region shows dead regions and red regions show overlap

3.3.3 Tiling evolution

In the beam tiling process described above, the generated tiling is valid for a single array configuration, frequency and epoch. When tracking positions that are not in a fixed frame with respect to the array, there are two important effects that alter the tiling. The first is the array projection, whereby the instantaneous UV coverage of the array changes with the position of the source, thus changing the PSF and therefore also the approximated beam shape. The second is parallactic angle rotation whereby beams with fixed celestial coordinates will orbit the array boresight due to the rotation of the Earth. This changing of both beam shape and position results in tilings becoming inefficient over time as the beams become more or less overlapped and the sampling of the desired tiling region becomes less uniform. Tiling efficiency as the fraction of the tiling area which is neither oversampled nor undersampled.
Re-tiling result in all beams changing their tracking positions and thus may

be problematic for observation types that require unbroken integration on specific positions. For long duration observations, it may be necessary to re-tile the beams as the current tiling becomes less efficient due to the changes in the beam shape. It is therefore useful to determine how long before a tiling generated at the start of that observation drops below some pre-defined efficiency.

Simulated observations start at timestamp t_0 with an optimized tiling. The beam shape is then updated with an interval δt (1 minute). At each update, a new beam shape is generated for that epoch and the resultant beams are positioned at the tiling coordinates from t_0. The tiling efficiency is then measured. If it exceeds the desired efficiency, the simulation will continue. If the target efficiency is not met anymore, the simulation is stopped and the time since t_0 is recorded as the tiling validity time.

3.4 Comparison of SPOTLIGHT and MeerKAT Code

While GMRT is a 30 antenna interferometer with a baseline of $\approx$ 25 km and collecting area $\approx$ 47713 m^2, MeerKAT is a 64 dish interferometer with a relatively smaller baseline of $\approx$ 8 km and collecting area of $\approx$ 9161 m^2. Due to the small baseline length of the array of MeerKAT, grating lobes do not significantly affect the beam parameters unlike the case in GMRT.

While, MeerKAT and GMRT both have 2 modes, viz. Survey Mode (Constant Overlap Mode) and Targeted Mode (Constant FoV Mode) and the basic algorithm remains the same, the different requirement based on the science goal and the engineering aspects causes both codes to have significant variations. MeerKAT operates in the higher frequency range, viz. 0.58 – 1.015 GHz, 0.9 - 1.67 GHz, 8 – 14.5 GHz while GMRT has 3 Bands in the lower frequency range 400 MHz, 700 MHz, 1200 MHz.

The code for SPOTLIGHT is developed in such a way, for the Targeted Mode, the overlap level is always greater than 0.5, the beam number is always less than a specific tolerance limit given by the user, and keeping these parameters fixed, the antenna configuration is varied to find the ideal beam parameters and fill the bounding box within the given tolerance number of

beams. Additionally, for both modes, it is ensured that the number of beams are a multiple of 24, because there are 24 processing units available for beam processing. It is ensured that GPU's are used to the fullest. The overlap level is slightly tuned from 0.5 and then the beam number is increased to keep it a multiple of 24. For the cases, where grating lobes are affecting the beam calculation, the overlap level is increased to 0.6.

On the other hand, the MeerKAT code let's the user select the antenna configuration, number of beams, FoV or overlap ratio depending on the mode. For constant FoV mode, it adjusts the overlap ratio without any upper or lower limit to fit the given number of beams in the bounding box. The constant overlap mode for MeerKAT works the same way as GMRT.
GMRT offers 3 types of bounding boxes for targeted mode, viz.

- Hexagonal
- Circular
- Rectangular (Square)

While, MeerKAT offers following bounding boxes.

- Hexagonal
- Circular
- Elliptical (only for constant FoV mode)
- Polygonal (only for constant FoV mode)

MeerKAT changes it's tiling when the efficiency of the tiling drops below a certain threshold.While, GMRT keeps the same tiling for the entire scan duration. However, both codes calculate a time for the best tiling and tiles according to it.

Chapter 4

Analysis

Standard RA-DEC Setup

- RA = 13 Hr 31 Mi 8.29 Sec
- DEC = 19° 30′ 33″
- Date = 15/11/2022
- Frequency = Band 3 Central Frequency : 400 MHz
- 30 Antenna Configuration

4.1 Beam arrangement

It was mathematically analysed, which of the tiling arrangement will be the best out of rectangular, shifted rectangular and hexagonal. Hexagonal packaging has the best packaging efficiency $\approx 82\%$ while, rectangular packaging (previously used) has around $\approx 78.5\%$ and shifted rectangular packaging has $\approx 81.5\%$ packaging efficiency. Considering computation efficiency, the shifted rectangular arrangement was chosen.

For rectangular arrangement, to calculate the efficiency we arrange 9 beams, the bounding box will be a rectangle with sides 6a and 6b, where a and b are the semi-major and semi-minor axis respectively. Area of a beam = πab Thus, the efficiency can be calculated as follows.

$$\text{Efficiency} = \frac{\text{Area inside beams}}{\text{FoV}} = \frac{9\pi ab}{36ab} = \frac{\pi}{4} = 78.5\% \tag{4.1}$$

For shifted rectangular arrangement, to calculate the efficiency, we arrange 7 beams such that the bounding box is a hexagon. Thus, the efficiency is calculated as follow.

$$\text{Efficiency} = \frac{\text{Area inside beams}}{\text{FoV}} = \frac{7\pi ab}{27ab} = 81.5\% \tag{4.2}$$

4.2 Analysis of Bounding Box Shapes

4.2.1 Analysis of Bounding Boxes

In the multi-beam former code, we have 3 various types of bounding boxes, viz. rectangular (square), hexagonal and circular as previously said in 3.2.2 and shown in figure 3.1, figure 3.2 and figure 3.3 In this analysis, it was analysed which of the 3 bounding boxes yield a better packaging efficiency, defined as follows.

$$\text{Efficiency} = \frac{\text{Number of beams} \times \text{Area of beam}}{\text{FoV}} \tag{4.3}$$

This analysis was done considering the Standard RA-DEC Setup alongside Band 3 frequency, 400 MHz and 17° elevation with 5 different total number of beams cases, varying from 24 to 2040. It was concluded from this analysis that code is working well for all the cases and giving expected results, i.e. an efficiency in the range 75-80 %. All the bounding boxes are equivalent in terms of efficiency.

4.2.2 Analysis of Tiling

Another analysis was done considering the hexagonal bounding box, for 3 elevations $(17°, 45°, 90°)$ and all 3 Bands (central frequency 400 MHz, 700 MHz, 1200 MHz) for 3 cases of total number of beam (24, 1000, 2000) as shown in figure 4.1, 4.2 and 4.3. From the analysis it was concluded that the packaging efficiency remains the same irrespective of the number of beams in a given bounding box.

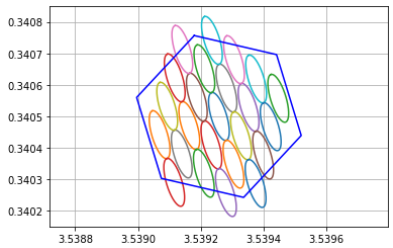

Figure 4.1: 24 Beams, Band 3 at Horizon

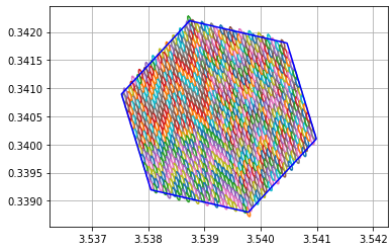

Figure 4.2: 1000 Beams, Band 3 at Horizon

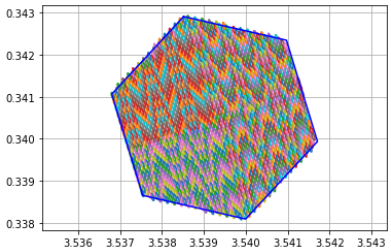

Figure 4.3: 2000 Beams, Band 3 at Horizon

4.3 Analysis of FoV

4.3.1 Analysis of FoV for 240 and 24 beams

The FoV is expected to decrease with elevation till 90° (staring from 17°). The decrease for band 3 is steeper than the decrease for band 4 and similarly, the decrease in band 4 is steeper than the decrease in band 5 evident in the plot 4.4. We are considering the Standard RA-DEC Setup.
The half power beam width (HPBW) will be minimum at the zenith (90° elevation), because of an almost circular beam, thus the effective field of view (summation of the area of beams) should be minimum at the zenith. The maximum and minimum FoV for 2040 beams and 24 beams at different band was analysed for Standard RA-DEC Setup and has been summarized in table 4.1.

The FoV requirement for the targeted mode was around 10 arcmin, considering 240 beams for Band 3 at zenith. Now these requirements were not

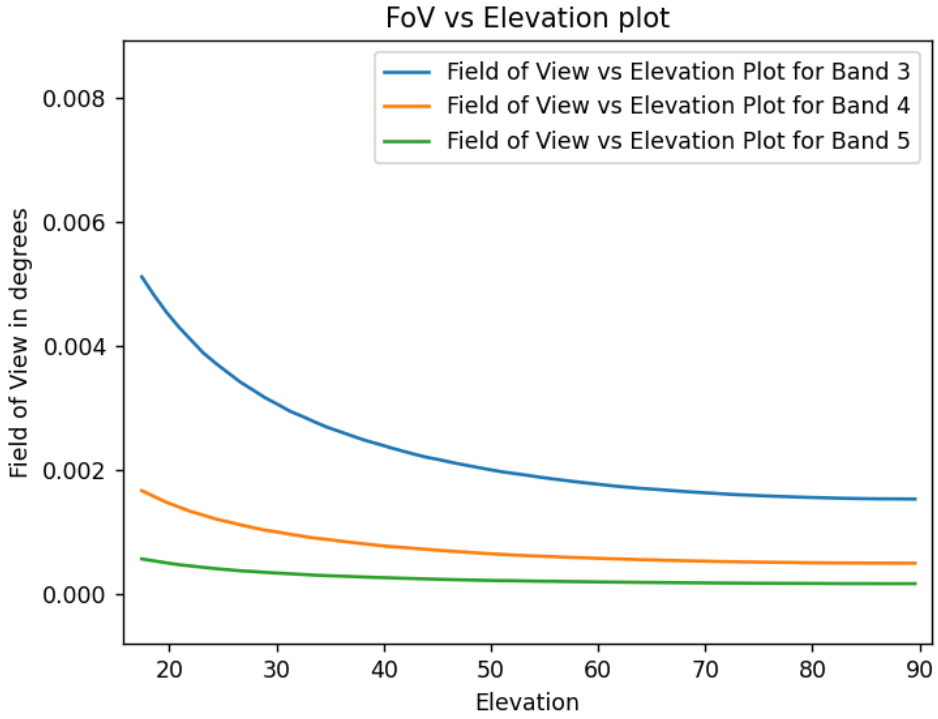

Figure 4.4: FoV vs Elevation

satisfied by the phased array beam at half power for 30 antennas, thus the analysis of FoV for lower antenna configuration was done. After analysis it was found that the requirement was not satisfied for even 23 antenna configuration.

4.3.2 Intrinsic Grating Lobes

For lesser than 23 antenna configuration, the issue with the power pattern was the presence of intrinsic grating lobes, the lobes had turning point above half power, thus at half power, they were non-detectable. Thus, the approximated ellipse at the half power had regions lesser than half power, which could affect the sensitivity and the localization of the target. This can be observed in figure 4.5. Thus, the overlap level was increased to extract the central contour as shown in figure 4.6, which reduces the FoV. After analysis, it was concluded that below 23 antenna configuration, the overlap level will be

	Band 3	Band 4	Band 5
Max FoV (2040 beams)	7.74 × 7.74 arcmin	4.43 × 4.43 arcmin	2.60 × 2.60 arcmin
Min FoV (24 beams)	0.84 × 0.84 arcmin	0.48 × 0.48 arcmin	0.28 × 0.28 arcmin

Table 4.1: Maximum and Minimum FoV for 30 antenna configuration

increased to 0.6, to extract the central contour and avoid regions lesser than 0.5 overlap.

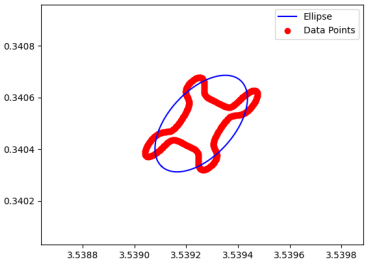

Figure 4.5: Ellipse fitted incorrectly for half power beam due to intrinsic grating lobes

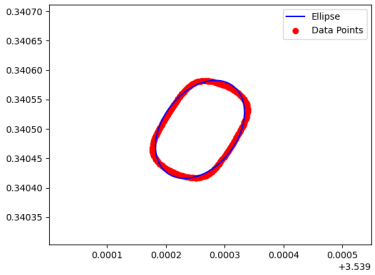

Figure 4.6: Fitted ellipse for 0.6 power beam, intrinsic grating lobes are removed.

4.3.3 Gaussian Extrapolation

To avoid the intrinsic grating lobes, we need to extract the central contour at higher overlap level, say around 0.9 and then fit the points to a Gaussian and extrapolate it further. Thus, we can obtain the actual HPBW. The power pattern is a 2D array, if we slice the array in the direction of beam orientation, then we will obtain a 1D array and 2D Gaussian plot. The HPBW of this Gaussian will be the major axis, similarly, if we slice the array perpendicular to the direction of beam orientation, then the HPBW of the Gaussian will be the minor axis. Thus, we can calculate the HPBW of the beam, using equation 4.4.

$$\text{HPBW} = \sqrt{\text{Major Axis}^2 + \text{Minor Axis}^2} \tag{4.4}$$

Antenna Number (Overlap Level)	Maximum Effective FoV (240 Beams)	Maximum FoV (240 Beams)	Minimum Effective FoV (24 Beams)	Minimum FoV (24 Beams)	Number of Beams for 10 arcmin
14 Antennas	26.53 x 26.53 arcmin	29.69 × 29.69 arcmin	8.39 x 8.39 arcmin	9.38 × 9.38 arcmin	48
15 Antennas (0.65 overlap level)	25.40 × 25.40 arcmin (14.99 × 14.99 arcmin)	28.40 × 28.40 arcmin (16.76 × 16.76 arcmin)	8.03 × 8.03 arcmin (4.74 × 4.74 arcmin)	8.98 ×8.98 arcmin (5.30 ×5.30 arcmin)	48 (96)
16 Antennas (0.55 overlap level)	19.60 × 19.60 arcmin (16.16 × 16.16 arcmin)	21.91 × 21.91 arcmin (18.07 ×18.07 arcmin)	6.20 × 6.20 arcmin (5.11 × 5.11 arcmin)	6.93 ×6.93 arcmin (5.71 × 5.71 arcmin)	72 (72)
17 Antennas (0.6 overlap level)	18.81 × 18.81 arcmin (11.52 × 11.52 arcmin)	21.03 × 21.03 arcmin (12.88 × 12.88 arcmin)	5.95 × 5.95 arcmin (3.64 × 3.64 arcmin)	6.65 × 6.65 arcmin (4.07 × 4.07 arcmin)	72 (144)
18 Antennas (0.6 overlap level)	17.81 × 17.81 arcmin (8.98 × 8.98 arcmin)	19.91 × 19.91 arcmin (10.04 × 10.04 arcmin)	5.63 × 5.63 arcmin (2.84 × 2.84 arcmin)	6.29 × 6.29 arcmin (3.18 × 3.18 arcmin)	72 (240)
19 Antennas (0.6 overlap level)	8.45 × 8.45 arcmin (7.25 × 7.25 arcmin)	9.45 × 9.45 arcmin (8.11 × 8.11 arcmin)	5.04 × 5.04 arcmin (2.29 × 2.29 arcmin)	5.63 × 5.63 arcmin (2.56 × 2.56 arcmin)	216 (360)
20 Antennas	8.00 × 8.00 arcmin	8.94 × 8.94 arcmin	2.53 × 2.53 arcmin	2.83 × 2.83 arcmin	312
21 Antennas (0.6 overlap level)	7.87 × 7.87 arcmin (5.31 × 5.31 arcmin)	8.80 × 8.80 arcmin (5.94 ×5.94 arcmin)	2.49 × 2.49 arcmin (1.68 × 1.68 arcmin)	2.78 × 2.78 arcmin (1.88 × 1.88 arcmin)	312 (672)
22 Antennas	5.81 × 5.81 arcmin	6.50 × 6.50 arcmin	1.84 × 1.84 arcmin	2.06 × 2.06 arcmin	576
23 Antennas	5.09 x 5.09 arcmin	5.69 ×5.69 arcmin	1.61 x 1.61 arcmin	1.80 ×1.80 arcmin	744
26 Antennas	3.48 x 3.48 arcmin	3.89 ×3.89 arcmin	1.10 x 1.10 arcmin	1.23 × 1.23 arcmin	1560
30 Antennas	2.35 x 2.35 arcmin	2.63 × 2.63 arcmin	0.74 x 0.74 arcmin	0.83 × 0.83 arcmin	3408

Figure 4.7: Antenna number, Effective and Actual Maximum and Minimum FoV and Maximum Number of Beams for required FoV

4.3.4 Analysis of Beams for 10 arcmin

An analysis for the number of beams required to reach the maximum FoV limit, viz. 10 arcmin was done for 30, 26, 23 till 14 antenna configuration at zenith as shown in figure 4.7. It was observed that the 10 arcmin and 240 beam limit reached for around 19 antenna configuration at 0.5 overlap level and 18 antenna configuration for 0.6 overlap level. However, the FoV was still less than 10 arcmin for 14 Antenna configuration considering 24 Beams. Thus, it was suggested to use a minimum of 48 beams for 10 arcmin FoV.

4.3.5 Effective FoV

The effective field of view is the area inside the beams, and the actual field of view is the area of the bounding box. This area is around 25% greater than the effective area. The figure 4.7 summarizes the number of beams for limiting FoV, maximum and minimum, effective and actual field of view. The antenna configuration used is the best antenna configuration, which yields the minimum grating lobes. A rigorous analysis for all possible antenna configurations is required to obtain the accurate overlap level.

4.4 Tiling Analysis

During a source observation, re-tiling has certain disadvantages as mentioned in 3.2.3. Thus, we arrange the beams according to a specific time. Thus in the best arrangement the beams should have the least drop in the effective FoV coverage during the observing session.

However, in the calculation of efficiency (here onwards efficiency in this term refers to effective FoV coverage) there is no consideration of overlapping beams, thus causing double counting of area when 2 beams overlap. However, this should not affect us from drawing the conclusion, the arrangement with the least efficiency should be the best arrangement as it will have the least overlap, thus the least double counted area.

The analysis of the Efficiency vs Time plot was done for 6 cases as follows. Beamshape corresponding to following time were used for tiling and to analysis its efficiency over the observing session.

1. Arrangement of the Start Time
2. Arrangement of the Mid Time
3. Arrangement of the End Time
4. Arrangement of the Mean of the HPBW
5. Arrangement of the Median of the HPBW
6. Arrangement of the RMS of the HPBW

It was obvious that the start time and end time arrangement will be the worst in terms of efficiency which was rightly proven by the analysis as well. As it can be observed in figure 4.8 and figure 4.9, the major and minor axes and thus, the HPBW follows a quadratic relation with time (Analysis time is 10:29 to 12:10 corresponding to El from 90 ° to 66 °) and hence the area of the gap between the beams will follows the 4^{th} order curve. Now according to figure 4.10, the efficiency follows a 4^{th} order relation with time (Analysis time is 5:18 to 10:29 to 15:18 (0 to 300 to 600 min on x-axis) corresponding to El from 17 ° to 90 ° to 22 °). So, the HPBW and efficiency are relatively related by a quadratic relation. Thus considering the Root Mean Square (RMS) of HPBW theoretically is the best option for the arrangement time.

As it can be observed in figure 4.8 and figure 4.9, the major and minor axes and thus, the HPBW follows a quadratic relation with time and according to figure 4.10, the efficiency follows a 4^{th} order relation with time, thus considering the RMS of HPBW theoretically is the best option for the arrangement time. Thus time corresponding to RMS of HPBW is the best time for tiling.

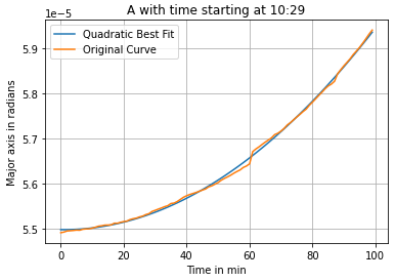

Figure 4.8: Major axis with time at 90° elevation

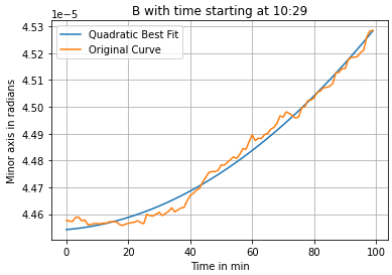

Figure 4.9: Minor axis with time at 90° elevation

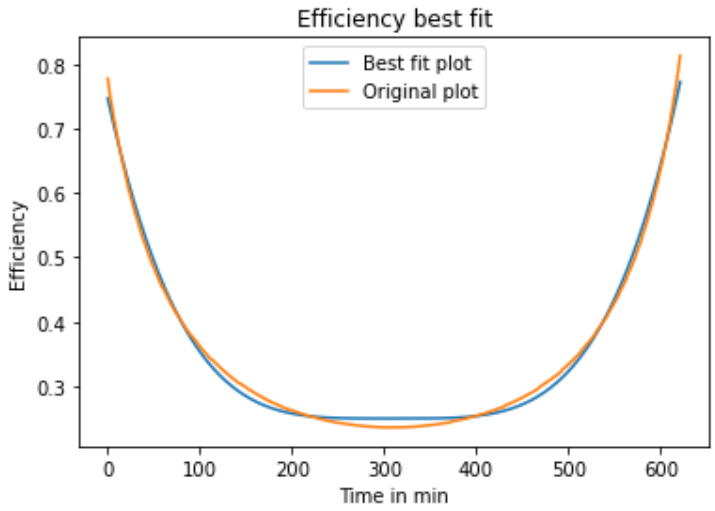

Figure 4.10: Efficiency plot for the entire duration fitted to 4th order curve

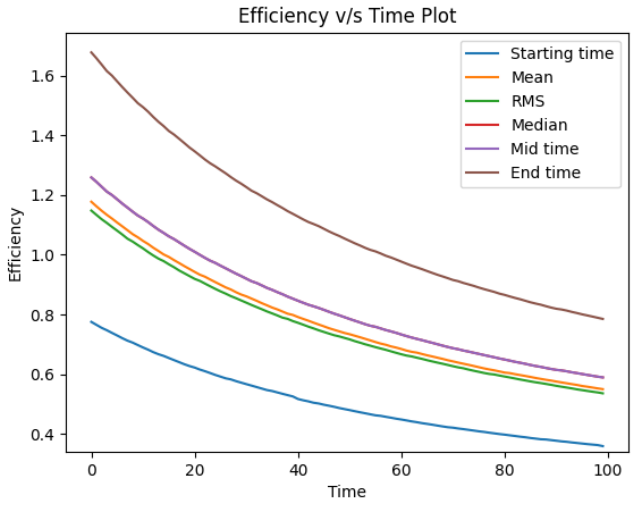

Figure 4.11: Efficiency vs Time plot for 0 to 100 min corresponding to 17° elevation to 90° elevation

Efficiency values above 0.8 indicate overlaps, while those below 0.8 show dead regions. As seen in the plot 4.11, the starting and ending times either have significant overlap or dead space, making them unsuitable arrangement times

as expected. The median and mid-time exhibit overlaps and have a higher overlap percentage with a lower percentage of dead regions compared to the mean and RMS. Similarly, the RMS shows greater overlap and fewer dead regions than the mean. Observing the plot, the distance between the tips at the start is greater than at the end. Thus, the lower the plot, the better the arrangement, making RMS the best option.

The efficiency tiling plot for 5 elevations was calculated and based on the plot it was concluded that the RMS (as suggested theoretically) is the best possible arrangement time. Conclusions drawn from plot 4.11 were valid for these 5 cases as well. In some cases, it was observed that the RMS and the HPBW mean seem to coincide, however the RMS was a better approximation than the Mean by a margin of 4.35%. This number was calculated using the starting efficiency and final efficiency of RMS and Mean.

Conclusion

The multibeam former code was updated in terms of features and mode. The packaging efficiency of the beams was increased from $\approx 78.5\%$ to $\approx 81.5\%$ by changing from rectangular to shifted rectangular arrangement. In addition to Survey mode, Target mode was developed.

Survey Mode
The survey mode or the constant overlap mode, it covers a broad FoV comparable to the primary beam-width. For the sky survey, around 2000 beams at overlap level around 0.5 are formed.

Target Mode
The target mode or constant FoV mode, it is used to observe targets like the globular cluster which are usually few arcmin in size. The number of beams processed are comparatively lesser (around 240). Based on the FoV, and tolerance on number of beams, keeping the overlap ratio near (above) 0.5, the beams are placed. If the FoV is still not satisfied then the antenna number is decreased to increase the beamwidth and thus, the FoV. It is ensured that number of beams are a multiple of 24, else the overlap level is tuned.

The FoV for the best fit antenna configuration for 30,26,23 till 14 antennas for 240 beams and 24 beams was analysed. The number of beams required for 10 arcmin was also analysed. For 30 antennas and 240 beams, the FoV was $2.35'$, while for 24 beams, the FoV was $0.83'$. Below 23 antennas due to the intrinsic grating lobes, the beam parameters were extracted incorrectly, thus the overlap level has been increased to 0.6 to extract the central contour.It was observed that the $10'$ and 240 beams were satisfied for 18 antennas at 0.6 overlap level. While, to satisfy $10'$ for 24 beams, the antenna number was lesser than 14 which was set as a lower limit.

It was observed that the efficiency is following 4^{th} order curve, and the HPBW follows in the 2^{nd} order curve wrt time. Thus after through analysis of 100 min for 5 elevations, the best time for the beam arrangement was found out to be the time of the RMS of the HPBW. The efficiency drop will be minimum during the observing session for this time arrangement.

Future Scope

1. Implementing an option for more bounding boxes which includes elliptical (observing spiral galaxies), polygonal, annulus and more depending on the specific need.

2. In this code, the beams are arranged in a shifted rectangular fashion, however, if the beams could be arranged in a hexagonal fashion using an efficient algorithm, it will reduce dead regions and help in localization of the FRB further,

3. To address the grating lobes issue, gaussian fit can be tried outThe coding part and the integration of the HPBW obtained using fitting and extrapolating Gaussian at higher overlap level has to done for obtaining precise beam parameters.

4. Currently, the code is considering uniform antenna amplitude gain, thus the beam is a sinc function, having significant grating lobes. However, if we consider changing the antenna amplitude gain say in the form of a Gaussian then, the grating lobes will be reduced, however the HPBW will increase. Implementation and analysis of this will be helpful.

References

1. Low Frequency Radio Astronomy - Jayaram N Chengalur, Yashwant Gupta, K. S. Dwarakanath (2007)
2. Wide field Beamformed Observation with MeerKAT
3. Analysing the impact of far-out sidelobes on the imaging performance of the SKA-LOW telescope
4. Simultaneous multi-telescope observations of FRB 121102
5. Injections and detections of FRBs for the SPOTLIGHT project with the GMRT
6. Internal STP Report on "Real-time Multi-beam Former Solutions Using C and Python" - Nishant Deo
7. Internal Report on "Optimal Beamforming for the GMRT" - Kshitij Agarwal
8. MeerKAT code GitHub page
9. Wikipedia
10. MATLAB Turorial on Youtube
11. Python
12. OpenCV Python Tutorials